

6th CIRP International Conference on High Performance Cutting, HPC2014

## Effect of Dressing on Internal Cylindrical Grinding

A. Daneshi<sup>a\*</sup>, N. Jandaghi<sup>a</sup>, T. Tawakoli<sup>a</sup>

<sup>a</sup>*Institute of Grinding and Precision Technology, KSF, Furtwangen University, Villingen-Schwenningen 78054, Germany*

\* Corresponding author. Tel.: +497720955776; fax: +497720955779. E-mail address: [dam@hs-furtwangen.de](mailto:dam@hs-furtwangen.de)

### Abstract

Performance of grinding operation is influenced by a variety of factors amongst which dressing process is the most important. Through the dressing process, the grinding wheel topography is produced. This affects, in turn, directly the grinding forces, workpiece surface quality and grinding wheel wear. This research aims to develop appropriate dressing strategies for small abrasive wheels in internal cylindrical grinding. For this purpose, three different dressing rollers, including an electroplated, a vitrified bond form roller and a cup-dresser, with four different grinding wheels, two CBN and two corundum wheels, were experimented. The studies on the ground surface roughness values and grinding forces prove the validity of the Schmitt-diagram in internal cylindrical grinding operations. When up-dressing, a finer workpiece surface was achieved as compared to the case of down-dressing. This is associated with higher grinding forces which are caused by the finer grinding wheel surface. Further investigation was carried out on the wear rate of CBN grinding wheels. However, no measurable wear was seen up to a specific material removal volume of 9700 mm<sup>3</sup>/mm.

© 2014 Published by Elsevier B.V. Open access under [CC BY-NC-ND license](https://creativecommons.org/licenses/by-nc-nd/4.0/).

Selection and peer-review under responsibility of the International Scientific Committee of the 6th CIRP International Conference on High Performance Cutting

*Keywords:* Internal Cylindrical Grindin; Schmitt-diagram, Dressing.

### 1. Introduction

The grinding process is usually considered as the finishing process in the manufacture of components with high accuracy and surface quality. The efficiency of grinding process is largely affected by conditioning and dressing of the grinding wheels owing to the topography which is created on their surface [1]. Through the dressing operation, the grinding process may be controlled in terms of the grinding forces, the grinding wheel wear, and workpiece surface roughness [2].

The basic relationships between the dressing parameters and grinding wheel topography were described by R. Schmitt and H. Scheidemann [3,4] (Fig.1). The effect of dressing speed ratio,  $q_d$ , and radial dressing feed,  $f_{rd}$ , on the grinding wheel surface topography is shown in Fig.1. The actual surface finish,  $R_{ts}$ , indicates the maximum difference between peak and valley on the grinding wheel surface. In other words, the higher  $R_{ts}$ , the rougher grinding wheel surface. Harbs [5] simulated the diamond grain paths in dressing of

superabrasive grinding wheels for internal grinding operation. The number of contacts of the diamond grains with the grinding wheel was simulated and its correlation with the variation of grinding wheel actual surface finish,  $R_{ts}$ , was determined.

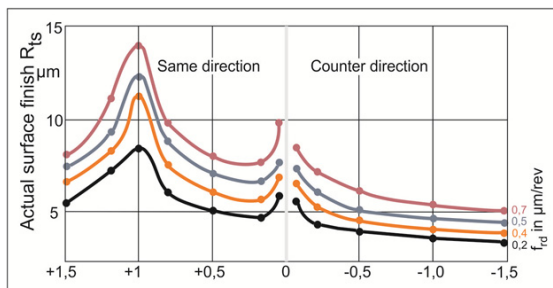


Fig. 1. The Schmitt-diagram shows the effect of dressing speed ratio and radial dressing in-feed on the grinding wheel surface roughness [3].

In this study, the effect of dressing parameters on the grinding output (grinding forces, workpiece surface roughness and grinding wheel wear) in internal grinding is discussed. The kinematics of the internal cylindrical grinding is identical to the external cylindrical grinding process between centers. Thus, the equations derived for the specific metal removal rate [6] were applied for internal cylindrical grinding in this paper. Nevertheless, there are different challenges when internal cylindrical grinding which make this process more difficult than external cylindrical operation. In the case of internal cylindrical grinding, the contact arc between the grinding wheel and workpiece is significantly larger than comparable external cylindrical grinding operations. Thereby, the removal of chips and a sufficient supply of cooling lubricant are difficult. In addition, during grinding of long holes of small diameters, there is a risk that the cantilevered spindle shaft is considerably deformed. In order to reduce the extreme deformations and minimize the resulting dimensional and form deviations sometimes long spark-out times are required. Fig. 2 illustrates a schematic of different phases occurring during internal cylindrical grinding operation.

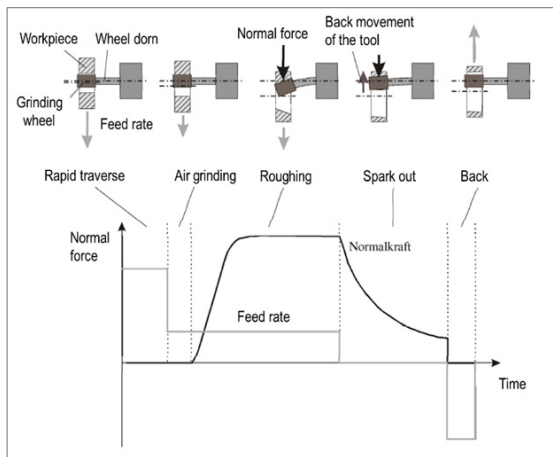


Fig. 2. Different phases of internal cylindrical grinding operation[7].

In dressing of small grinding wheels, because of the small diameter and high spindle speeds, such that typically used in internal cylindrical grinding operations, the generally recommended values of the overlap ratios cannot be achieved. In addition, the contact frequency of the diamond grains with the grinding wheel and flattening of the active path curves are strongly influenced by the diameter ratio, the ratio of the dressing roller diameter to the grinding wheel diameter [8]. Therefore, in general only a compromise between the topography of the grinding wheel to be produced and process efficiency can be achieved. This means, for instance, that utilizing a vitrified dresser may be a way to reach a stronger abrasive removal than using of metal bonded dressers, but these types of dressers are subject to high wear and high batch variation.

This research aims to find the effect of dressing roller and dressing parameters on the workpiece surface roughness and

grinding forces in the case of small grinding wheels through the internal cylindrical grinding experiments.

## 2. Methodology

In this investigation, a ceramic and a galvanic bonded dressing rollers were used to dress the grinding wheels. Within the variable parameters of dressing, the maximum cross feed rate of the dresser is of particular interest. The result of dressing is verified by the analysis of the grinding wheel topography, as well as, proper (internal cylindrical) grinding tests. Based on this should be discussed approaches for the effective generation of an optimal grinding wheel topography and possibly verified by practical tests.

## 3. Experimental Setup



The experiments were conducted on a CNC cylindrical grinding machine manufactured by EMAG-Karstens, type HG 204. The workpiece from hardened bearing steel 100Cr6 (1.3505) with 60 HRC was selected for the experiments. This material is mainly used for producing components being under high stress (good rigidity and high wear resistance, such as bearings and bearing rings). Four vitrified bonded grinding wheels, two CBN and two corundum wheels (Table 1), with the dimensions 30x20x12 (DxBxH) were used.

Table 1. The specifications of the grinding wheels used in the experiments

Wheel	Code	Grain size [ $\mu\text{m}$ ]	Bond
CBN	B91	91	Vitrified
CBN	B64	64	Vitrified
Corundum	F80	180	Vitrified
Corundum	F150	80	Vitrified

Dressing operations were carried out by two diamond form rollers with different bonds. The specifications of the dressing tools are listed in Table 2.

Table 2. Two different diamond rollers were used to dress the grinding wheels.

Code	Bond	Dimension[mm] (DxBxH)	Photo
D426	Galvanic	120 x 13 x 40	
D107	Vitrified	120 x 13 x 40	

For the force measurement on the workpiece, the rotating four component dynamometer manufactured by Kistler was used. In order to measure the surface roughness and the surface topography of the ground workpieces, a roughness and contour measuring device (Hommel Tester T8000, Hommel Etamic GmbH) was used. In addition, this device has been used to determine the grinding wheel radial wear. In order to measure the grinding wheel wear, an indirect method was selected. The wheel profile is ground and mapped on a steel plate and the generated profile is measured.

**4. Results and Discussion**

The initial experiments were carried out under following operational parameters:

- Dressing with different speed ration,  $q_d = \pm 0,4; \pm 0,6; \pm 0,8$
- Dressing depth of cut,  $a_{ed}, 3 \times 2 \mu\text{m}$  for CBN and  $3 \times 5 \mu\text{m}$  for Corundum wheels
- Dressing feed rate: Maximum 50% of the grinding wheel abrasive grit size per revolution
- Plung grinding operation
- Grinding speed ration  $q_s \approx 30-45$
- Specific material removal rate  $Q'_w = \text{max.} 15 \text{ mm}^3/\text{mm}\cdot\text{s}$

Through initial experiment, the following parameters were selected and used in all dressing operations to reach the optimum process conditions in terms of the form accuracy, burning, chatters and machine vibrations:

- Cutting speed:  $v_c = 60 \text{ m/s}$
- Speed ration:  $q_s = 33.7$
- Specific material removal rate:  $Q'_w = 10 \text{ mm}^3/\text{mm}\cdot\text{s}$
- Spark out time: 2s

**4.1. Effect of Dressing Speed Ratio**

Grinding forces and workpiece surface roughness may be controlled by changing the dressing speed ration because variation of this parameter has a great influence on the grinding wheel topography. In the figures 3-6 the experimental conditions and the measured specific grinding forces and ground workpiece roughness values against the dressing speed ration,  $q_d$ , are shown. The profile of the so-called Schmitt-diagram can be seen in the following diagrams, wherein the roughness was measured on the ground workpiece. As expected, the grinding forces and workpiece roughness have an inverse relationship that means the finer the ground surface, the higher the grinding forces.

As shown in figures 3 and 4, the typical Schmitt diagram is valid in the case of internal cylindrical grinding with CBN wheels. It is valid for both CBN grain sizes and both case of dressing with galvanic and vitrified dressing rollers. The typical behaviors of the surface roughness and grinding forces against dressing speed ration are seen in these diagrams. The up dressing results in finer surface and higher grinding forces. This is due to the higher number of the diamond grits which come into contact with the grinding wheel abrasive grains and therefore, finer topography on the grinding wheel surface is generated. Thus the number of the active grains increases.

This leads to finer surface roughness and higher grinding forces.

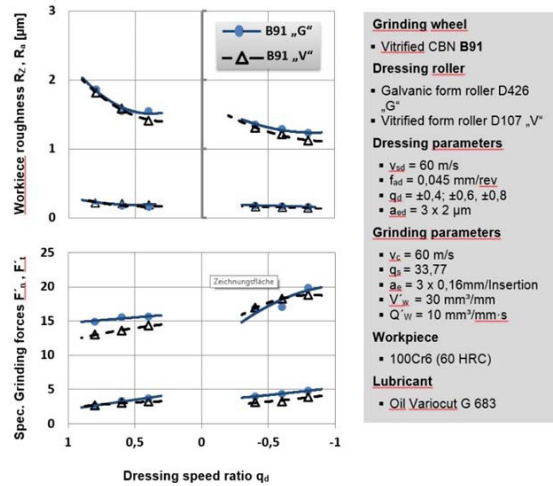


Fig. 3. Effect of the dressing speed ratio,  $q_d$ , on the workpiece surface roughness and grinding forces in dressing of small CBN grinding wheel B91 with diameter 30mm.

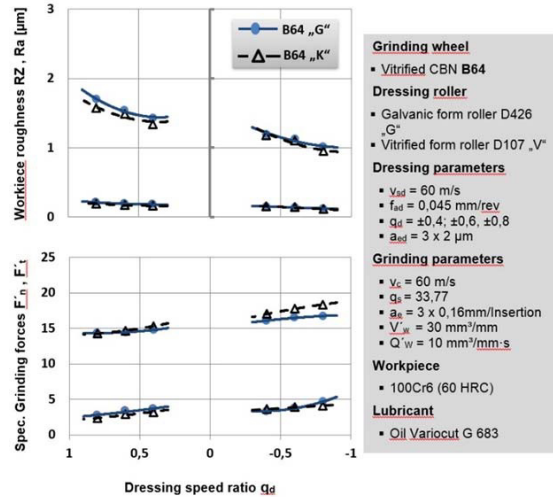


Fig. 4. Effect of the dressing speed ratio,  $q_d$ , on the workpiece surface roughness and grinding forces in dressing of small CBN grinding wheel B64 with diameter 30mm.

Figures 5 and 6 illustrate how the dressing speed ratio influence on the grinding parameters when working with corundum grinding wheels. Like those for CBN wheels, the Schmitt-diagram behavior is validated by these figures for corundum wheels with two different grain sizes and dressing conditions, one dressed by galvanic roller and another one by ceramic roller. Two corundum wheel with grain size  $180\mu\text{m}$  (F80) and  $80\mu\text{m}$  (F150) were used. As expected, the finer surfaces were achieved when grinding by the wheel F150.

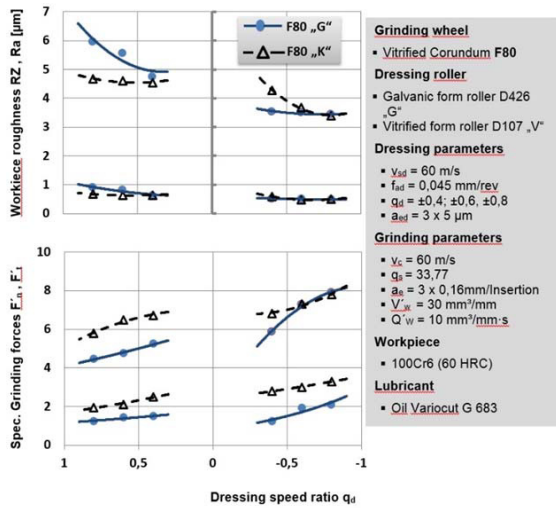


Fig.5. Effect of the dressing speed ratio,  $q_d$ , on the workpiece surface roughness and grinding forces in dressing of small corundum grinding wheel F80 with diameter 30mm.

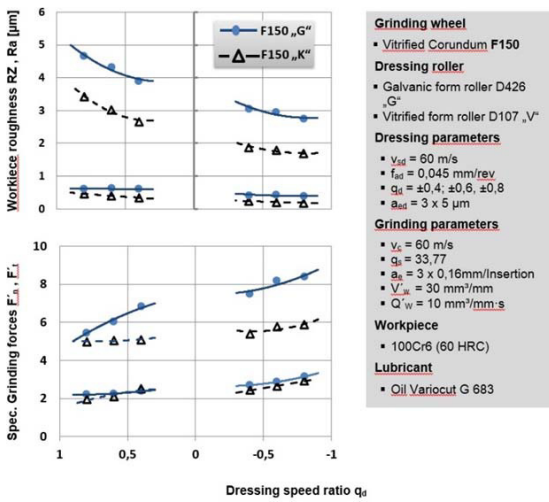


Fig.6. Effect of the dressing speed ratio,  $q_d$ , on the workpiece surface roughness and grinding forces in dressing of small corundum grinding wheel F150 with diameter 30mm.

4.2. wear behavior of the vitrified bonded CBN (B91)

For the determination of wear of the CBN abrasive wheel, long-term experiments were carried out. The grinding wheel was dressed with the same parameters as in Figure 3. Only half of the grinding wheel width was used in grinding operation and therefore a step was formed on the wheel surface. After a certain time, the form of grinding wheel surface was mapped on a steel plate by its grinding. The step on the steel plates was measured and used and the grinding wheel radial wear indicator. Despite the high-resolution measuring system, profile measurement of the steel plate and the microscope in the whole series of experiments, it was

hardly possible to determine the wear value after removal volume  $V'_w = 9700 \text{ mm}^3 / \text{mm}$ . Therefore, a radial wear of  $<1$  micron is assumed. Under the microscope, only one edge wear of the grinding wheel could be detected.

4.3. Long Term Experience of the Vitrified Bonded CBN (B91)

In Figure 7, the behavior of the surface roughness and specific grinding normal forces in different material removal volume is shown after up dressing of the grinding wheel ( $q_d = -0.5$ ). As it is seen, the grinding normal force is high at the beginning of the process and the surface roughness value is low. However, with increasing material removal, the grinding force dramatically falls and the surface roughness becomes worse. This happens because the pores of the bond after dressing are relatively closed. After a certain cutting volume, the pores become gradually open and the binding is reset. In Figure 8 left, the surface of the grinding wheel after dressing is illustrated. Figure 8 right shows the same grinding wheel after removal volume of  $9700 \text{ mm}^3/\text{mm}$ . The variation of the bond in this case can clearly be seen. As it is seen in Fig.7, the normal forces increase after 6000 removal volume. This is contributed to the chip loading.

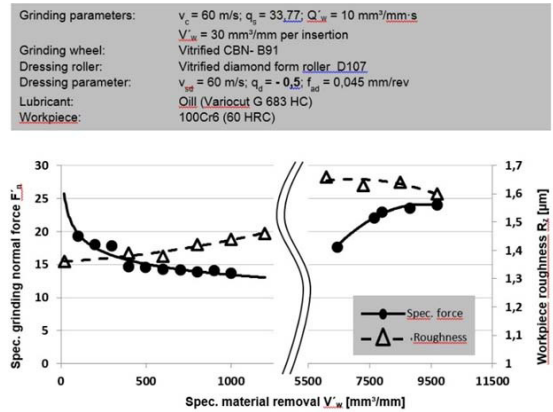


Fig. 7. the behavior of the surface roughness and specific grinding normal forces in different material removal volume ( $q_d = -0.5$ )

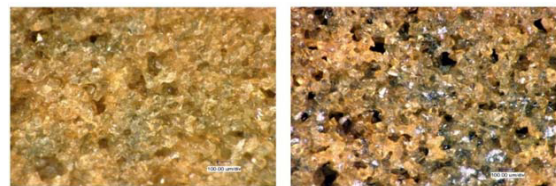


Fig.8. Illustration of the grinding wheel surface under a microscope at a 175x magnification. (Left): grinding wheel after dressing (Right): grinding wheel after  $V'_w = 9700 \text{ mm}^3/\text{mm}$ .

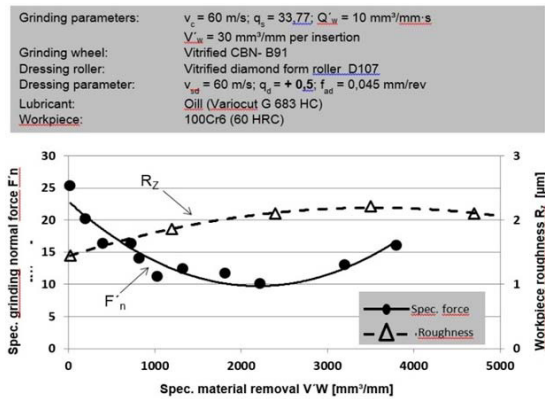


Fig.9. the behavior of grinding process in long term experiments when the grinding wheel is dressed in down dressing mode ( $q_d = +0.5$ )

Figure 9 illustrates the behavior of grinding process in long term experiments when the grinding wheel is dressed in down dressing mode ( $q_d = +0.5$ ). Like Fig. 7, the grinding forces are relatively high at the beginning of the process because of the closed pore and reduce gradually with appearing open pores

## 5. Conclusion

This research is concluded as follows:

- The dressing and internal cylindrical grinding experiments with small vitrified CBN and corundum grinding wheels show that the Schmitt diagram is valid for small diameter grinding wheels. The dressing were carried out in both down and up dressing modes and Schmitt diagrams were verified in both modes.
- The measurement of radial wear of the ceramic CBN grinding wheel after a long term experiment showed that the wear value of this wheel after removal volume of 9700 mm<sup>3</sup>/mm is negligible (less than 1 µm).
- Measurement of the topography of the CBN wheel shows that the grinding wheel after dressing is closed and need to cut a certain volume of material to become open. This leads to high grinding forces right after dressing. However, the forces decrease after a certain removal volume.
- When using the small vitrified grinding wheels, sharpening or using relatively low feed rates after dressing at the beginning of the process is recommended. This is carried out to open the grinding wheel pores or resetting the bond material.

## Acknowledgments

The authors would like to thank “Tyrolit Schleifmittelwerke K.G.”, “KREBS & RIEDEL GmbH & Co.”; and “HERMES Schleifkörper GmbH & Co.” for fruitful cooperation. Furthermore, financial support by VDS (Verband Deutsche Schleifmittelwerke) is gratefully acknowledged.

## References

- [1] Tawakoli, T.; Westkämper, E.; Rabeiy, M, 2007, Dry grinding by special conditioning, International Journal of Advanced Manufacturing Technology, 33: 419-424.
- [2] Tawakoli, T.; Rasifard, A.: Dressing of Grinding Wheels, in “Machining with Abrasives” edited by M. J. Jackson and J. P. Davim, Springer-Verlag New York, 2011, ISBN 978-1-4419-7301-6.
- [3] Schmitt R.: Abrichten von Schleifscheiben mit diamantbestückten Rollen. Thesis TU Braunschweig 1968
- [4] Scheidenmann H.: Einfluß der durch Abrichten mit zylindrischen und profilierten Diamantrollen erzeugten Schleifscheiben-Schneidfläche auf den Schleifvorgang. Thesis TU Braunschweig 1973
- [5] Harbs U.: Beitrag zur Einsatzvorbereitung hochharder Schleifscheiben. Thesis TU Braunschweig 1996
- [6] König W.: Fertigungsverfahren Band 2 – Schleifen, Honen, Läppen; 2. Auflage, VDI-Verlag Düsseldorf, 1989, ISBN 3-18-400810-X
- [7] Straßburger, S.: Prozessüberwachung, -diagnose und -optimierung bei Innenrundsleifen mittels aktiver Magnetlager; Dr.-Ing. Dissertation, Technische Universität Darmstadt, 2003
- [8] N.N.: Konditionieren von Schleifwerkzeugen (Grindology Paper C4), Firmenschrift Tyrolit Schleifmittelwerke Swarovski K.G.